

Supplementary Data

Clinical-Grade Stem Cell-Derived Retinal Pigment Epithelium Patch Rescues Retinal Degeneration in Rodents and Pigs

Ruchi Sharma^{1#}, Vladimir Khristov^{2#}, Aaron Rising^{2#}, Balendu Shekhar Jha¹, Roba Dejene¹, Nathan Hotaling¹, Yichao Li³, Jonathan Stoddard⁴, Casey Stankewicz⁵, Qin Wan², Connie Zhang², Mercedes Maria Campos⁶, Kiyoharu J. Miyagishima², David McGaughey⁷, Rafael Villasmil⁸, Mary Mattapallil⁹, Boris Stanzel¹⁰, Haohua Qian³, Wai Wong¹¹, Lucas Chase⁵, Steve Charles¹², Trevor McGill⁴, Sheldon Miller², Arvydas Maminishkis², Juan Amaral¹³, and Kapil Bharti^{1*}

1 Unit on Ocular and Stem Cell Translational Research, National Eye Institute, NIH, Bethesda, MD

2 Section on Epithelial and Retinal Physiology and Disease, National Eye Institute, NIH, Bethesda, MD

3 Visual Function Core, National Eye Institute, NIH, Bethesda, MD

4 Casey Eye Institute, Oregon Health & Science University, Portland, OR

5 Cellular Dynamics International, Inc. - A FUJIFILM Company - Madison, WI

6 Histology Core, National Eye Institute, NIH, Bethesda, MD

7 Ophthalmic Genetics and Visual Functional Branch, National Eye Institute, NIH, Bethesda, MD

8 Flow Cytometry Core, National Eye Institute, NIH, Bethesda, MD

9 Laboratory of Immunology, National Eye Institute, NIH, Bethesda, MD

10 Macula Center Saar, Sulzbach Knappschaft Eye Clinic, Sulzbach/ Saar, Germany

11 Unit on Neuron-Glia Interactions in Retinal Disease, National Eye Institute, NIH, Bethesda, MD

12 Founder, Charles Retina Institute, Germantown, TN 38138

13 Office of Scientific Director, National Eye Institute, NIH, Bethesda, MD

Equal first

*Corresponding Author - Kapilbharti@nei.nih.gov

MATERIALS AND METHODS

Research and clinical-grade iPSC derivation, maintenance, and RPE differentiation

Reporter iPSC line expressing GFP under the control of TYROSINASE enhancer and constitutive RFP was previously published (54) and used to optimize the research-grade differentiation protocol. iPSCs were cultured on MEFs for 4 days before using for differentiation. To make cell aggregates, iPSCs were treated with Collagenase for 20 mins. After collagenase was aspirated, NEIM (DMEM/F12, KOSR, supplemented with N2, B27, LDN-193189 10uM, SB431452 10 nM, CKI-7 hydrochloride 0.5 uM, and IGF-1 1ng/ml) was added to the wells (1ml/well) and cell scarper was used to scrape the colonies. Cell aggregates were grown in 10 cm² low attachment corning dishes in NEIM medium for 48 hrs. After 48 hours, floating cell aggregates were collected and seeded in matrigel coated plates in RPEIM (DMEM/F12, KOSR, supplemented with N2, B27, LDN-193189 100uM, SB431452 100 nM, CKI-7 hydrochloride 5 uM, and IGF-1 10ng/ml, PD0325901 1uM) and cultured for 3 weeks. After 3 weeks in RPEIM, cells were moved to RPECM (DMEM/F12, KOSR, supplemented with N2, B27, Nicotinamide 10mM and Activin A 100ng/ml) for 3 more weeks with regular medium change. Pigmented patches of immature RPE cells were collected through differential trypsinization and seeded on to transwells or T-25 flasks in RPEGM (MEM, Sigma; 1% N2 supplement, ThermoFisher; 1% Glutamine, ThermoFisher; 1% non-essential amino acids, ThermoFisher; 125 mg Taurine (Sigma)/500 ml; 10 ug Hydrocortisone (Sigma)/500 ml; 0.0065 ug Triiodo-thyronin (Sigma)/500 ml; 5% FBS, Sigma) (32). Table S3 provides a list of all reagents used in the manufacturing process. Flow cytometry was performed to check GFP expression in the differentiating cells at various time points.

For clinical-grade protocol, feeder free iPSCs clones were derived from CD34⁺ PBMC using a previously published report (17). Working banks of up to eight clones were validated for pluripotency by flow cytometry, sterility (WuXiApp Tech), normal G-band karyotyping (Cell Line Genetics), STR identity (Univ. Madison Clinics), plasmid loss (Cellular Dynamics Inc.), and oncogene sequencing (Q2 Solutions). iPSCs cells were then seeded on vitronectin (A14701S, ThermoFisher) coated surface in E8 Medium (A1517001, ThermoFisher). After 2 days, cells were transferred to RPEIM for 10 days and then

to RPECM for another 10 days. On day 22, cells were switched to RPEGM, trypsinized at day27 and reseeded in RPEGM. On day 42, cells were enriched using anti-CD24 and anti-CD56 antibodies and reseeded on to scaffolds in RPEMM (MEM, Sigma; 1% N2 supplement, ThermoFisher; 1% Glutamine, ThermoFisher; 1% non-essential amino acids, ThermoFisher; 125 mg Taurine (Sigma)/500 ml; 10 ug Hydrocortisone (Sigma)/500 ml; 0.0065 ug Triiodo-thyronin (Sigma)/500 ml; 5% FBS, Sigma; 50 uM PGE2, R&D Biosystems).

Real time PCR

Total RNA was isolated using NucleoSpin RNA (#740955, Machery-Nagel) per manufacturer's protocol. RNA was quantified using an ND- 1000 spectrophotometer (Nanodrop Technologies). cDNA synthesis and custom made 24 RPE gene array plates were purchased from Bio-rad. Sybr green based Qpcr was run on ViiA 7 Real-Time PCR System (Thermo Fisher Scientific) according to manufacturer's protocol. Each sample were run in at least 3 biological replicate and data was analyzed in R-based software.

Trans Epithelial Resistance

Electric intactness was measured using EVOM2 and EndOhm chamber (World Precision Instruments) and each clone was measured for its resistance for 3 biological replicates.

Hexagonality measurement methodology

Cells were fixed in 4% paraformaldehyde and stained for Anti-Zonula Occluden-1 (ZO1) conjugated to AlexaFluor 594. Whole trans-wells were mounted and 2mm x 4mm x 60 micrometer sections of each well were imaged at 20x with a Zeiss Axio Scan-1. Z-stacks were then maximum-intensity projected (MIP) and cells in the MIP were analyzed for their borders in MATLAB. Once cell borders had been identified a binary "mask" was created to measure cell morphological properties. How close RPE were to an ideal convex regular hexagon was measured using a metric known as "Hexagonality". Briefly, Hexagonality was assessed by taking 10 times the average of two different ratios (Eq. 3). The two ratios

are the hexagon-side-ratio (HSR) as defined by Eq. 1 and the hexagon-area-ratio (HAR) as defined by Eq. 2.

$$\text{Eq. 1: } \frac{P_{Cell}}{P_{Hull}} * \left[1 - \left| 1 - \frac{P_{cell}}{6 * \sqrt{\frac{4 * A_{cell}}{6 * \cot(\frac{\pi}{6})}}} \right| \right] = HSR$$

$$\text{Eq. 2: } \frac{A_{Cell}}{A_{Hull}} * \left[1 - \left| 1 - \frac{4 * A_{cell}}{6 * \left(\frac{P_{cell}}{6}\right)^2 * \cot(\frac{\pi}{6})} \right| \right] = HAR$$

$$\text{Eq. 3: } 10 * \left(\frac{HSR + HAR}{2} \right) = \text{Hexagonality}$$

In the above P_{Cell} is the perimeter of the cell, P_{Hull} is the perimeter of the convex hull surrounding the cell, A_{Cell} is the area of the cell, A_{Hull} is the area of the convex hull.

Phagocytosis of Photoreceptor Outer Segments

Phagocytic ability of iRPE cells was measured using a published protocol with slight modifications (55). Bovine photoreceptor outersegments (POS) (InVision Bio) were labeled with pH-rodo dye (ThermoFisher) as per manufacturer's protocol. Mature iRPE cells after 5 weeks of culture on transwells or PLGA scaffolds were fed at the concentration of 5 POS/iRPE cell for 4 hours at 37C. Cells were washed with DPBS 3 times and incubated in 0.25% trypsin for 20 minutes. Trypsinized cells were collected with 1 ml pipette and suspended in 15 ml tube containing 10 ml of RPE MM. 15 ml tubes with cells were centrifuged at the 400g for 5 minutes, the cell pellet was washed 3 times in 10 ml of DPBS, resuspended in 10 ml DPBS and the cell suspension was passed through a 0.44um cell strainer. Cells samples were run through MACS Miltenyi Flow Cytometer. Live cells were selected as DAPI negative. A laser channel with an excitation at 586 nm and emission at 515 nm was used to determine fluorescence from uptaken pH-rodo labelled POS. Flow cytometry data was analyzed with flowjo

software and the median fluorescence for channel Y1 positive population was calculated for the fed and unfed samples. The ratio of fed samples to unfed samples was calculated and plotted in a graph.

Lactic Acid Measurements

PLGA scaffolds were incubated under the same conditions used for culturing of iPSC-RPE-patches. Culture medium was changed every alternate day and incubated medium was collected in a 15 ml tube. Media from three consecutive medium changes was combined in one tube. Same procedure was followed for all of the six technical replicates. Collected medium was immediately frozen and stored at -80 C. Lactic acid measurements were performed at the Certified NIH Clinical Center Clinical Chemistry lab. Since each technical replicate tube from three consecutive media collections contained 12 ml of medium, it was lyophilized to reduce the total volume. Lyophilized material was resuspended in 1 ml of 1x D-PBS. Lactic acid measurement was performed at the NIH Clinical Center General Chemistry lab using using a Lactate Gen. 2 machine with a measuring range of 0.2-15.5 mmol/L (1.8-140 mg/dL).

Oncogene Coding Variant Analysis

Coding regions and near exonic positions across 223 oncogenes were deeply sequenced by Q² Solutions for each iPSC clone and accompany PBMC donor. Variants labeled as potentially deleterious were detected using Tute Genomics in the Q² provided variant call file (VCF). Additionally, we used three different somatic callers (Mutect version 1.15, SomaticSniper version 1.0.5.0; and Strelka version 1.0.15) to compare each iPSC clone to the matched PBMC. This parallel analysis found no new mutations in exon or splice positions. All sequences can be downloaded from dbGAP server (ID: SUB4785176).

Animals

Castrated Yucatan minipigs (RRID: NSRRC_0012) and Yorkshire pigs (age: 5-11 months ; weigh: 30-40 Kg), Crl:NIH-Foxn1^{tmu} immunocompromised and Royal College of Surgeon rats were used. All animal studies were reviewed and approved by the NIH Animal Care and Use Committee. All animals were handled in accordance with the Association for Research in Vision and Ophthalmology (ARVO)

statement for the use of animals in Ophthalmic and Vision Research. All animals were fed according to the body weight.

Surgical Delivery of Cells in Rodents

Suspension

Post-natal day (P) 21-28, RCS rats (RRID: RGD_1358258) or adult immunocompromised rats, Crl:NIH-*Foxn1*^{nu} Nude rats (RRID # RGD_2312499) were anesthetized with 2, 2, 2-Tribromoethanol (intraperitoneal; 230 mg/kg; Sigma) and eyes received topical 0.5% proparacaine HCl anesthesia. Pupils were dilated with 1% tropicamide and 2.5% phenylephrine HCl and the eye was slightly proptosed. A small scleral/choroidal incision (~1 mm) was made 2 mm posterior to the limbus in the dorso-temporal region using increasing gauge needle tips. A small lateral corneal puncture was made using a 30-gauge needle to limit increase of intraocular pressure and reduce efflux of cells following injection. Two microliters of suspension containing the total cell dose (100,000 cells) was delivered into the subretinal space of one eye using a fine glass pipette (internal diameter, 75–150 μ m) inserted into the subretinal space. The conjunctiva was then repositioned over the scleral incision. All animals included in the study received injection of cells with a minimum pre and post dose cell viability of 90%. All RCS rats received daily intraperitoneal injections of dexamethasone (1.6 mg/Kg) for 2 weeks post cell transplantation to minimize a potential inflammatory response.

iRPE-patch

Placement of the iRPE-patch followed the same general procedure as with suspension injection with the following exceptions. Subretinal blebs were created using 2-3 μ l balanced salt solution (BSS+) and scleral incision was extended using an 18ga needle to accommodate insertion of a 1-mm round implant. Using a sterile trephine, a 1-mm punch of RPE-scaffold was extracted from the culture plate. Using ILM peel forceps, the 1-mm implant was grasped at the distal end to offer protection and stability to the scaffold during implantation. Forceps were gently inserted into the subretinal space in the orientation of RPE facing the photoreceptors.

Optokinetic Tracking

Optokinetic tracking (OKT) thresholds were measured using a virtual optomotor system (VOS; CerebralMechanics) that allows evaluation of both the left and right eyes independently. Thresholds were evaluated at P90, using methods described elsewhere (39, 56). A single principle operator evaluated thresholds that were confirmed by a second operator.

Immunosuppression

Tetracycline antibiotics Doxycycline and Minocycline are used orally in doses of 5mg/Kg twice a day. A loading intramuscular dose of methylprednisolone is used at doses of 5mg/Kg, followed by similar daily oral single doses of prednisone. Rapamycin is used orally with a loading dose of 2 mg, followed by a 1 mg daily dose. Tacrolimus is used in oral doses of 0.5 mg/day.

Laser-injury Model

An IQ 532 micropulse laser (Iridex) with a TxCell scanning laser delivery device is used to selectively damage the RPE using a Volk HR centralis contact lens (Volk Optical Inc.) with 74° field of view, 1/08x magnification and laser spot magnification of 0.93x. Micropulse power sufficient to obtain a mild whitening of the lasered area (1000-1600 milliwatts), and exposure times of 330 milliseconds are used. With micropulse duty cycles of 1% (0.100 milliseconds pulse “on” and 9.900 milliseconds pulse “off”) and a spot size of 200 microns, 7x7 confluent grids are made to create a 49 mm² lesion.

Pig iRPE-patch Transplantation

Sterilization of the surgical area with povidone iodine, a temporal canthotomy, superior rectus traction and nictitating membrane retraction is performed to increase the surgical exposure area. A nasal peritomy is done to expose sclera and 4 surgical ports (infusion, chandelier illumination, and 2 working ports) are created 3.5mm from limbus using 25G valve trocar cannulas (Alcon surgical). After vitrectomy and posterior vitreous detachment, a localized retinal detachment (RD) is done in the visual streak (laser area)

using a 25G/38G cannula (MedOne Surgical Inc.) and scissors retinotomy is done at the base of the RD. A sclerotomy (2.3-2.5 mm) is done in the area of the nasal port to accommodate the transplantation tool. Tip of the tool is introduced through the retinotomy into the subretinal space where the iRPE scaffold is released with the help of the viscous fluid injector device of the vitrectomy system (Alcon surgical). An ocular wound clamp (custom made) closes the sclerotomy to maintain the intraocular pressure while performing fluid air exchange to flatten the detached area which is confirmed by intraoperative OCT. The sclerotomy is closed with nylon 8-0.

Optical Coherence Tomography and Fluorescein Angiography

After the animal is adequately anesthetized, a Jet-Electrode was placed on the eye with an appropriate amount of GenTeal Tears (Alcon). OCT was performed using Spectralis (Heidelberg Engineering) with a 55° degree lens. The region of interest (ROI) was placed in the center and both averaged single B-scan across ROI and volume OCT scans covers entire ROI was performed. Follow-up function of the instrument was used to allow for OCT scans at the same retinal location for each examine time point. Spectralis was also used for capturing fluorescein angiogram with intravenous injection of Sodium Fluorescein (SF, Akorn Inc, Lake Forest, IL). Early (first min) and late phase (15 min) angiograms were recorded.

Multi-focal Electroretinography

mfERG was recorded using the RETImap system (Roland Consult). Briefly, a bipolar contact lens (The GoldLens Corneal Electrode) was placed on the eye. A ground electrode, Genuine Grass Platinum Subdermal Needle Electrode (Natus Manufacturing Limited) was placed under the skin of the chin of the animal. A minimum of 3 cycles were used for each recording and a total of 3 overlapping retinal regions were measured. In each recording the ROI was shifted slightly around the field of view to account for slight differences in optics. A low bandpass of 10hz and a high bandpass of 300hz was used. The 7 mfERG components determined from the MATLAB program are N1 (first major trough)

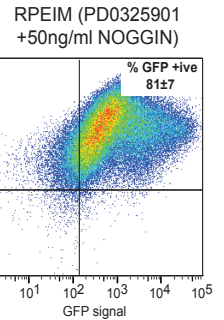
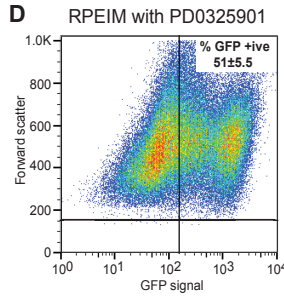
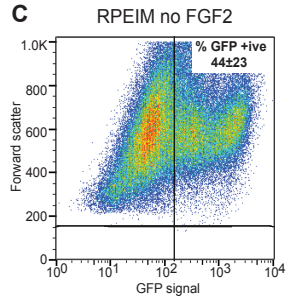
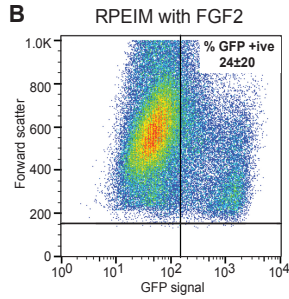
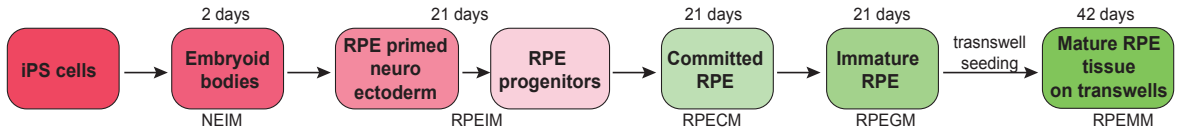
and P1 (the following peak) amplitudes (nV/deg²), N1P1 (difference between N1 and P1 amplitudes), Scalar Product, AUC, and widths of N1 and P1 (time in msec at half the max amplitude of peak). The 7 mfERG components are normalized by subtracting the laser signal of the implant with the healthy region signals and dividing by the pre-laser signal.

Immunostaining and Histology

Tissue preparation for immunohistochemistry was done by placing the eye in 4% PFA for a maximum of 4 hours after enucleation. The surgery area was dissected out and placed in 10% sucrose/PBS overnight followed by 24 hours in 20% sucrose/PBS. The samples were then placed in a 2:1 OCT:20% Sucrose solution and flash frozen in a cryostat mold and placed in the -80 freezer until sectioning on the cryostat could be performed. Cryostat sectioning was done at 10µm sections with tissue section separated every 50 µm. Immunohistochemistry was performed in general as follows: 5% Natural Goat Serum (NGS) (Thermo Fisher Scientific) blocking solution for 2 hrs followed by primary antibody incubation overnight in 1% NHS at room temperature. Primary antibodies include: RPE65 (1:300, Abcam; ab78036, and custom antibody from M. Redmond lab/NEI 1:400), Biotinylated Peanut Agglutinin (PNA) (1:300, Vector Laboratories; B-1075), STEM121 (1:300 Takara Clontech; Y40410), STEM101 (1:300, Takara Clontech), Rhodopsin (1:10,00, Encor Biotechnology Inc.; MCA-B630); Red/Green Opsin (1:300 Millipore; AB5405); Blue Opsin (1:300 Millipore; AB5407); iPSCs - OCT4 (#653704, Biolegend, RRID: AB_2562018), TRA 1-81 (#560124, BD Biosciences); and SSEA-4 (#560126, BD Biosciences); RPE progenitors - MITF (#X2397M, Exalpa), PAX6 (#PRB-278P, Covance); committed RPE - PMEL17 (#HMB45, Dako), TYRP1 (#NBP2-32901, Novus Biologicals), and mature RPE - BEST1 (#NB300-164, Novus Biologicals). Ezrin (#E8897, SigmaAldrich), Collagen IV (#ab6311, Abcam), ALDH1A3 (#ab80176, Santa Cruz Biotechnology). Following

overnight incubation, the tissue samples were washed 3x in 1% NGS solution and secondary antibodies conjugated to fluorescent markers, Alexa 488, Alexa 555 and or Alexa 633 (Thermo Fisher Scientific), to the appropriate primary in 1% NGS solution at 1:300 dilution. The slides were then either imaged on the Zeiss 800 confocal microscope or the Zeiss Axio Scan. Z1 slide scanner. The number of nuclei (DAPI) in the implant region (either empty scaffold or iRPE-Patch) was normalized to the corresponding healthy region on the same section. The same distance across the retina (~ 400 μm) was used for the implant area and the corresponding healthy area to count.

A Research-grade triphasic RPE differentiation protocol (107 days)



F Percent GFP positive cells in RPECM with:

ACTIVIN A - (A)	69 ± 16
Nicotinamide +ACTIVIN A - (NA)	81 ± 7
WNT3a (W)	83 ± 8.5
Nicotinamide + ACTIVIN A + WNT3 (NAW)	82 ± 10

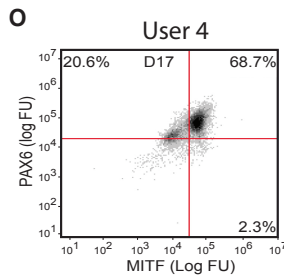
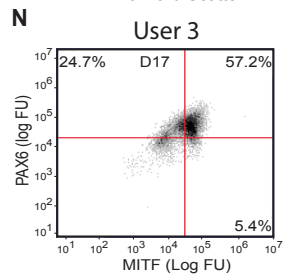
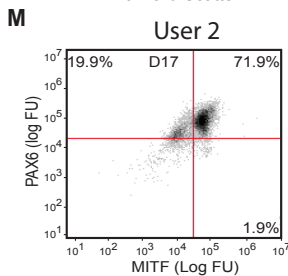
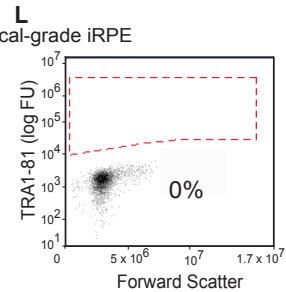
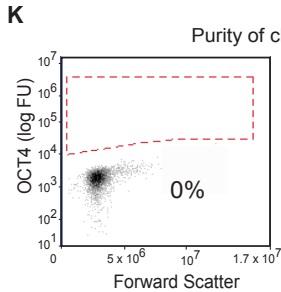
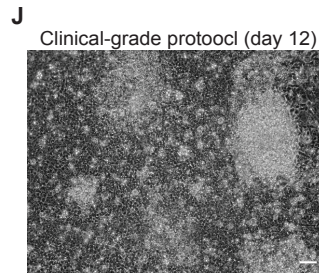
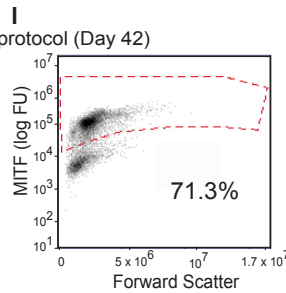
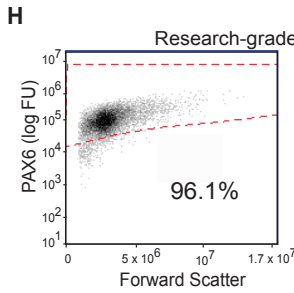
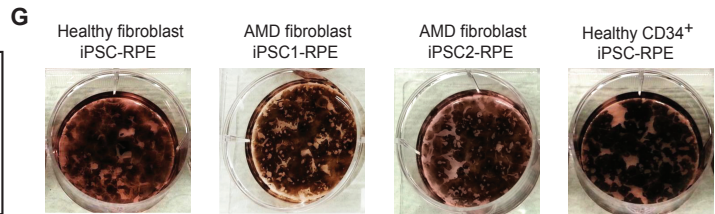
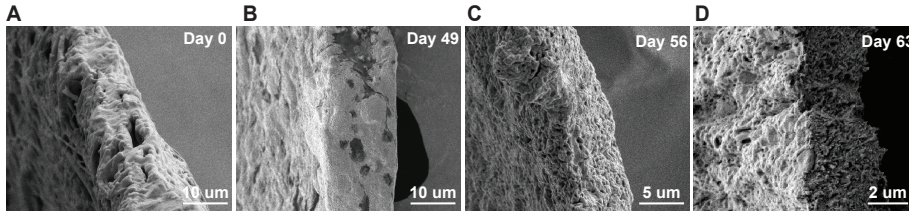


Fig. S1. Optimization of iPSC-RPE differentiation. (A) Time-line for research-grade iPSC-RPE differentiation. Differentiation into mature RPE takes 107 days and is initiated using 3D iPSC aggregates in NeuroEctoderm Induction Medium (NEIM). (B, C) Expression of RPE-specific GFP in iPSCs differentiated in the presence of FGF2 (B) or without FGF2 (C). GFP expression is measured using a reporter iPSC line expressing GFP under the control of TYROSINASE gene promoter⁴². (D) iPSC-RPE differentiation in the presence of MEK inhibitor (PD0325901) in RPEIM. (E) iPSC-RPE differentiation in using DUAL SMAD-inhibition with low amounts of NOGGIN (50ng/ml) in RPEIM combined with ACTIVIN A (100ng/ml) in RPE Commitment Medium (RPECM). (F) ACTIVIN A and WNT3a in RPECM do not show any synergistic increase in number of GFP-positive RPE progenitors, as shown recently¹⁵ (n=3). (G) Reproducible maturation of RPE derived using a research-grade differentiation protocol from healthy and patient iPSC lines (fibroblasts or blood derived) (n=4). (H, I) Flow cytometry analysis of PAX6 and MITF positive RPE cells at D42 of research-grade differentiation protocol. (J) Epithelial phenotype in cells on D12 of clinical-grade differentiation protocol. (K, L) Flow cytometry analysis of OCT4 and TRA1-81 at D42 of clinical-grade iPSC differentiation protocol confirms the absence of iPSCs. (M-O) Three additional users (first user data in Fig. 1D) reproduced the clinical-grade iPSC differentiation protocol, shown by flow cytometry analysis of PAX6 and MITF double positive cells at D17.

In vitro degradation of PLGA scaffolds - side view



In vitro degradation of PLGA scaffolds - top view

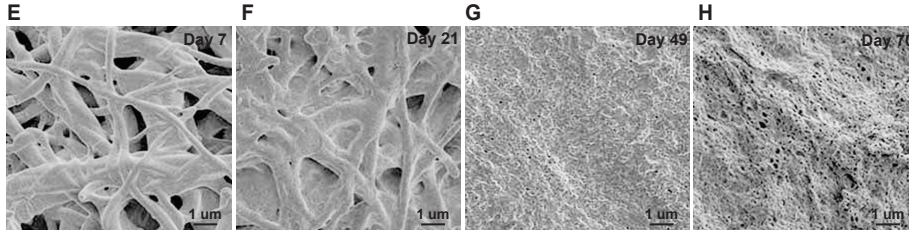


Fig. S2. Degradation Kinetics of PLGA Scaffold. (A-H) SEM images of PLGA scaffold from an edge (A-D) and *en face* (E-H) views during degradation, showing changes in surface topology and thinning of the entire scaffold due to bulk degradation of PLGA fibers.

Supplementary Figure 3

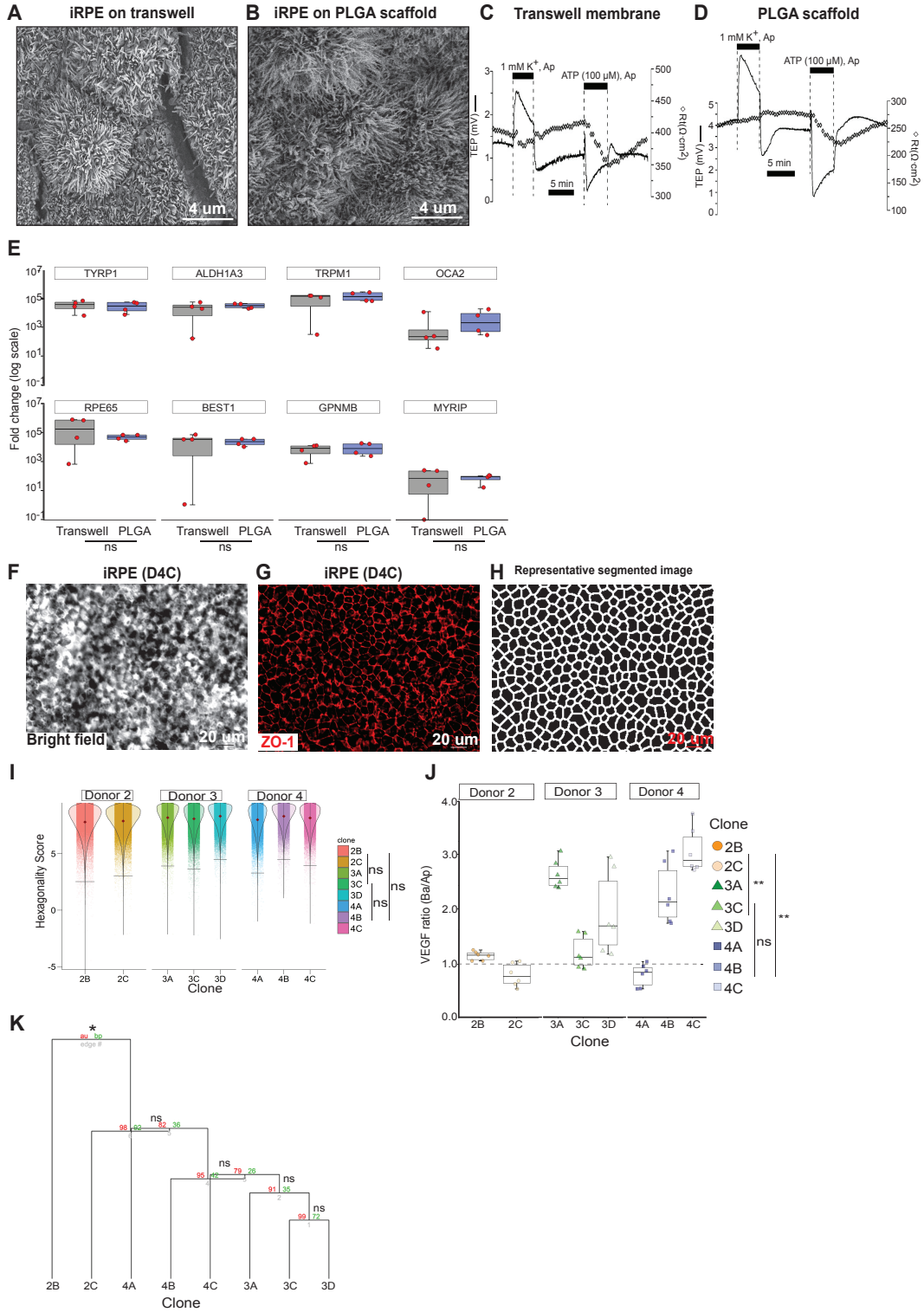


Fig. S3. Evaluation of functionally mature iRPE patch. (A, B) SEM confirms the presence of comparable apical processes on PLGA-iRPE-patch and transwell-iRPE-patch. (C, D) Electrophysiological traces confirm similar electrical properties of the PLGA-iRPE-patch and transwell-iRPE-patch. (E) Comparison of fold change in RPE-specific genes between PLGA-iRPE-patch and transwell-iRPE-patch as compared to iPSCs showed similar level of monolayer maturity on the two substrates. (n=3). ANOVA was performed to determine comparability between iRPE on scaffolds and transwell; p-value=0.237 (F, G) Bright field and ZO-1 (red) immunostained images of iRPE from AMD donor 4, iPSC clone C (D4C). (H) ZO-1 immunostained images are segmented using a convolutional neural network to highlight cell borders. Segmented images were used for morphometric analysis. (I) Morphometric analysis performed on ZO-1 stained images of iRPE-patches from all three AMD donors using REShAPE software. 75,000-100,000 cells are imaged per patch and images analyzed to determine the hexagonality score (how hexagonal is the cell) of each RPE cell. Data is displayed as violin plots with the center dot representing the mean and horizontal lines in each plot representing 99% data points. RPE-patch derived from different clones are differently colored (n=8). p-values: Dunn's test was therefore used for reporting multiple pairwise comparisons after a Kruskal-Wallis test for stochastic dominance among k groups was performed. 2B/2C- 3A/3C/3D=0.061; 2B/2C-4A/4B/4C=0.174; 3A/3C/3D-4A/4B/4C=0.757 (J) Graph shows the polarized VEGF secretion (basal/apical ratio) for different AMD-iRPE-patch (n=8). Dunn's test was performed to compare iRPE from different donors: p-values: 2B/2C-3A/3C/3D=0.005; 2B/2C-4A/4B/4C=0.006; 3A/3C/3D -4A/4B/4C =1 (K) Bootstrap hierarchical cluster for PCA of all iRPE from three donors shows samples that are similar and different from each other.

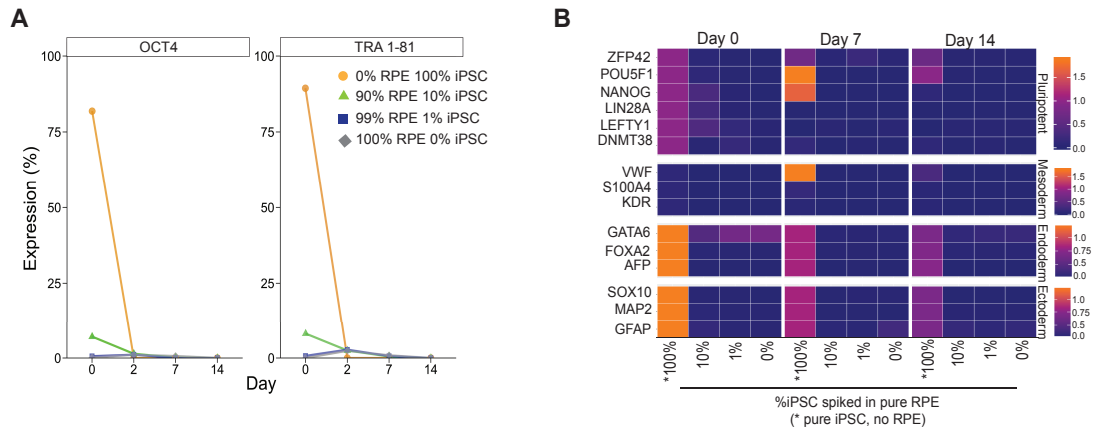


Fig. S4. Assessment of iPSC-survival in iRPE cultures. (A, B) *In-vitro* spiking studies performed by seeding mixed cultures of iPSC and RPE on scaffolds (100% iPSC; 10% iPSC+90%RPE; 1% iPSC+99%RPE; and 100% RPE). iPSC-markers (OCT4 and TRA 1-81) were evaluated at days 0, 2, 7, and 14 post seeding by flow cytometry (A). Gene expression analysis of iPSC (ZFP42, OCT4, NANOG, LIN28A, LEFTY1, DNMT38) and lineage-specific markers (mesoderm – VWF, S100A4, KDR; endoderm – GATA6, FOXA2, AFP; non-RPE ectoderm – SOX10, MAP2, GFAP) evaluated at days 0, 7 and 14 days post-seeding of mixed iPSC, RPE cultures. Data is displayed as heat maps of relative Δ CT values. All values are normalized to day 0 data (B). This experiment confirms that PLGA scaffolds and RPE maturation medium do not support iPSC or non-RPE lineage growth. Non-RPE lineage genes are not expressed in iRPE-cells.

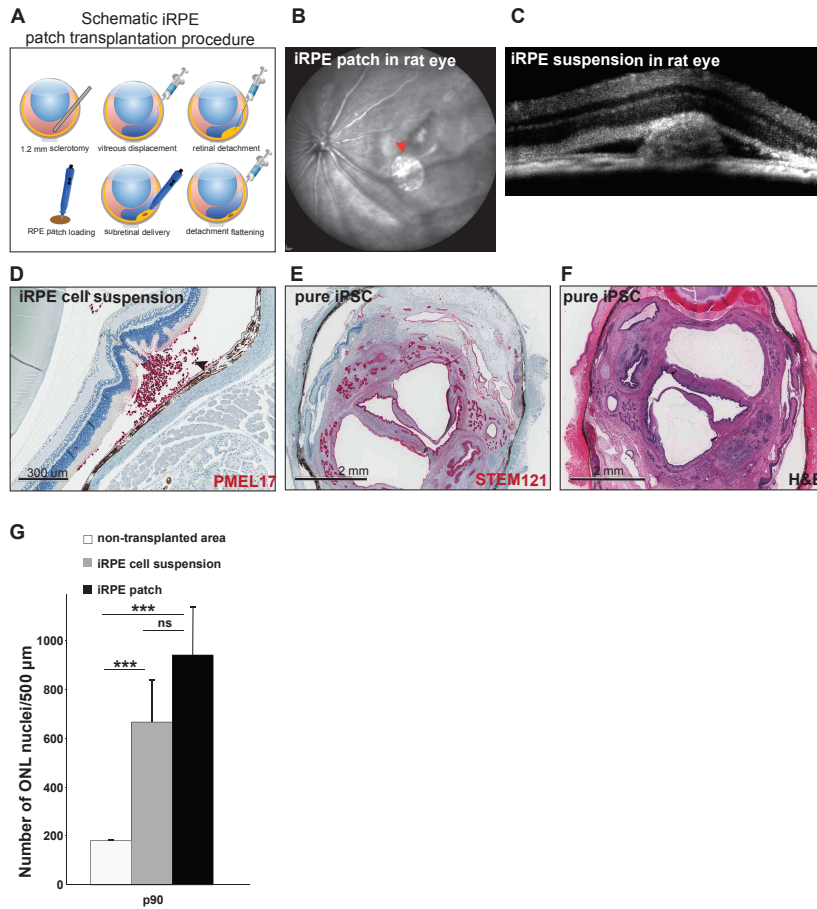


Fig. S5. Safety and efficacy assessment of iRPE patch in rodents (A) Schematic of 0.5 mm diameter iRPE-patch transplantation in rat sub-retinal space. Surgery starts with a 1.2 mm sclerotomy, followed by vitreous displacement with hyaluronic acid (HA), retinal detachment by HA injection in the sub-retinal space, iRPE-patch loading in the transplantation tool, delivery of the patch in the sub-retinal space, and flattening of retinal detachment by hyaluronic acid. (B) Visualization of successfully transplanted iRPE-patch in the sub-retinal space of a rat eye. (C) OCT shows transplanted iRPE-suspension in the sub-retinal space of a rat eye. (D-F) Immunohistochemistry for human-specific PMEL17 (red, D) confirms RPE phenotype of injected AMD iRPE cells suspension in the sub-retinal space at 10 weeks post-injection. In contrast, injected human iPSC suspension (STEM121 – red, E) leads to teratoma formation (F) n=10 (3 formed teratoma). (G) Quantification of number of nuclei in the outer nuclear layer (ONL) of RCS rat retina above the area of transplant as compared to the non-transplanted area of the same eye.

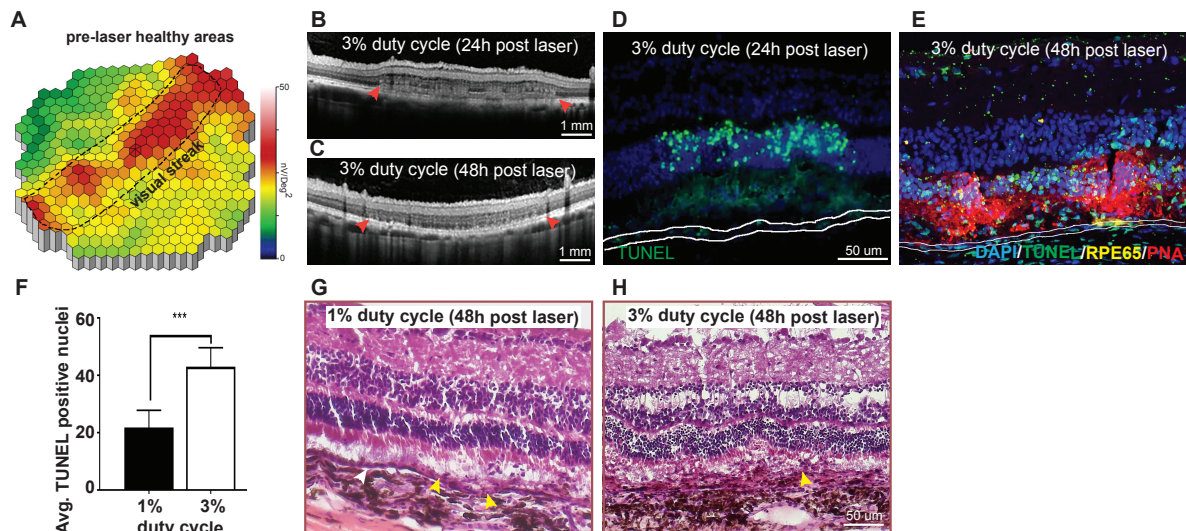


Fig. S6. Optimization of laser-induced RPE injury in pig eyes. (A) heatmap showing the average mfERG electrical waveforms responses of the pig eye before the laser was performed. Laser ablation of RPE is performed in the highest electrical activity area, the visual streak (dotted line) of the pig eye. (B, C) OCT of 3% laser duty cycle at 24 and 48 hours post-laser shows RPE and ONL damage and sub-retinal edema (red arrowhead). (D) 3% duty cycle laser area staining with TUNEL (Green) and DAPI (Blue) shows several apoptotic cells in the ONL at 24h. White line shows the RPE monolayer. (E) At 48h, with 3% duty cycle laser, both ONL and RPE are severely damaged, with several apoptotic cells (green) and weak PNA (red) and RPE65 (yellow) staining. (F) Average TUNEL positive ONL nuclei in 1% and 3% laser duty cycle laser damage retina were measured. N=3. (G, H) H &E staining of the 1% (G) and 3% (H) duty cycles laser after 48hours. Healthy area is evident to the left in the 1% duty cycle (G, white arrowhead). Note, disrupted photoreceptors in 3% laser as compared to 1% (yellow arrowheads).

Supplementary Figure 7

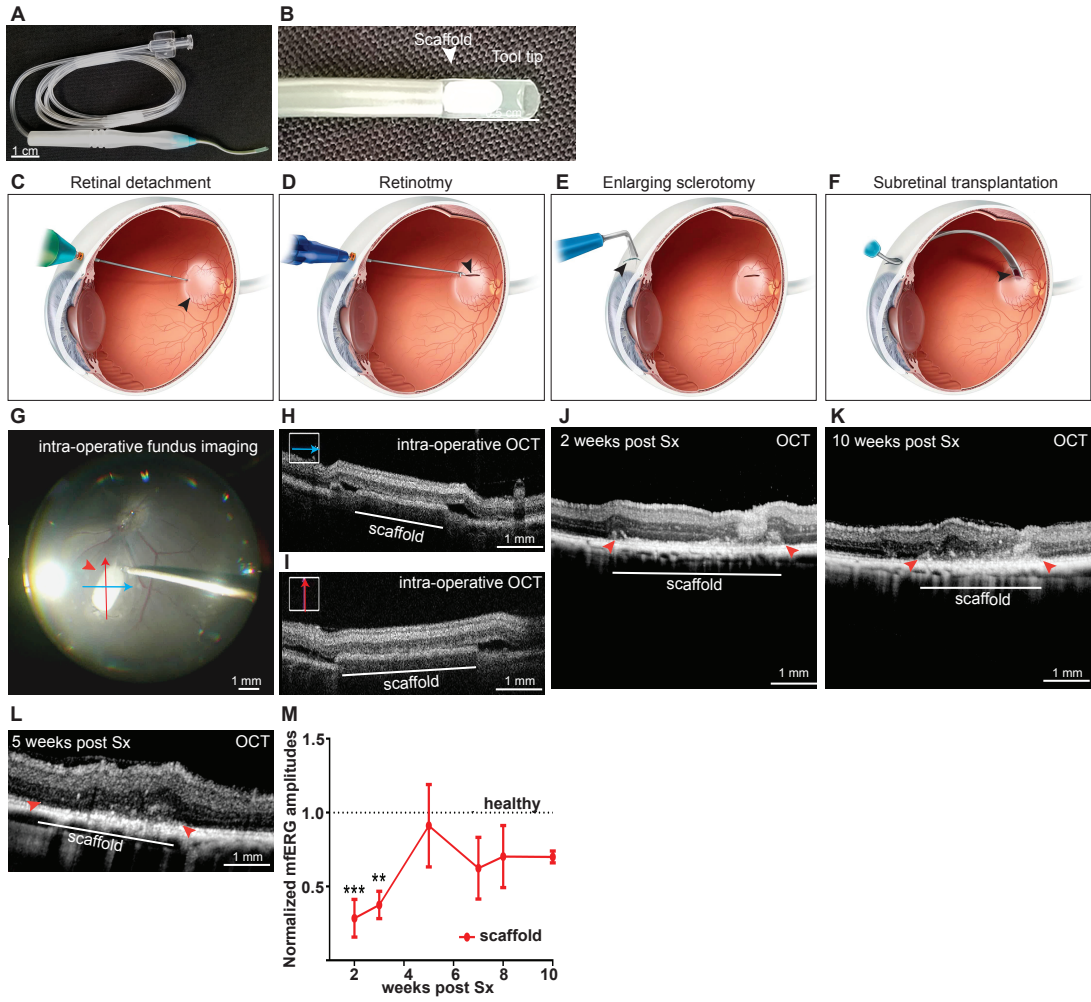


Fig. S7. Optimization of sub-retinal transplantation procedure in pigs. (A, B) Image of transplantation tool and the tool tip loaded with an empty-scaffold (arrowhead). (C-F) Schematic of the pig surgery. After a standard four port-vitreotomy, retina is detached using a 38G blunt tip cannula (C), followed by retinotomy (D), enlarging of the sclerotomy (E), and delivery of the human RPE-patch in the sub-retinal space (F). (G-I) Intra-operative fundus imaging and optical coherence tomography (iOCT) performed during surgery confirm delivery of the 4x2 mm scaffold at the intended sub-retinal location. (J-L) OCT of pig eyes two (J), ten weeks (K), five weeks (L) post-surgery confirm empty scaffold degradation in non-immunosuppressed pigs and no inflammation caused by degrading PLGA byproducts. (M) N1P1 mfERG signal over the empty-scaffold shows a significant reduction until week 3, caused likely by the surgical procedure. The signal recovers over time as the surgical damages heals and the scaffold degrades (2-way ANOVA, $p < 0.0001$) $n = 3$.

Supplementary Figure 8

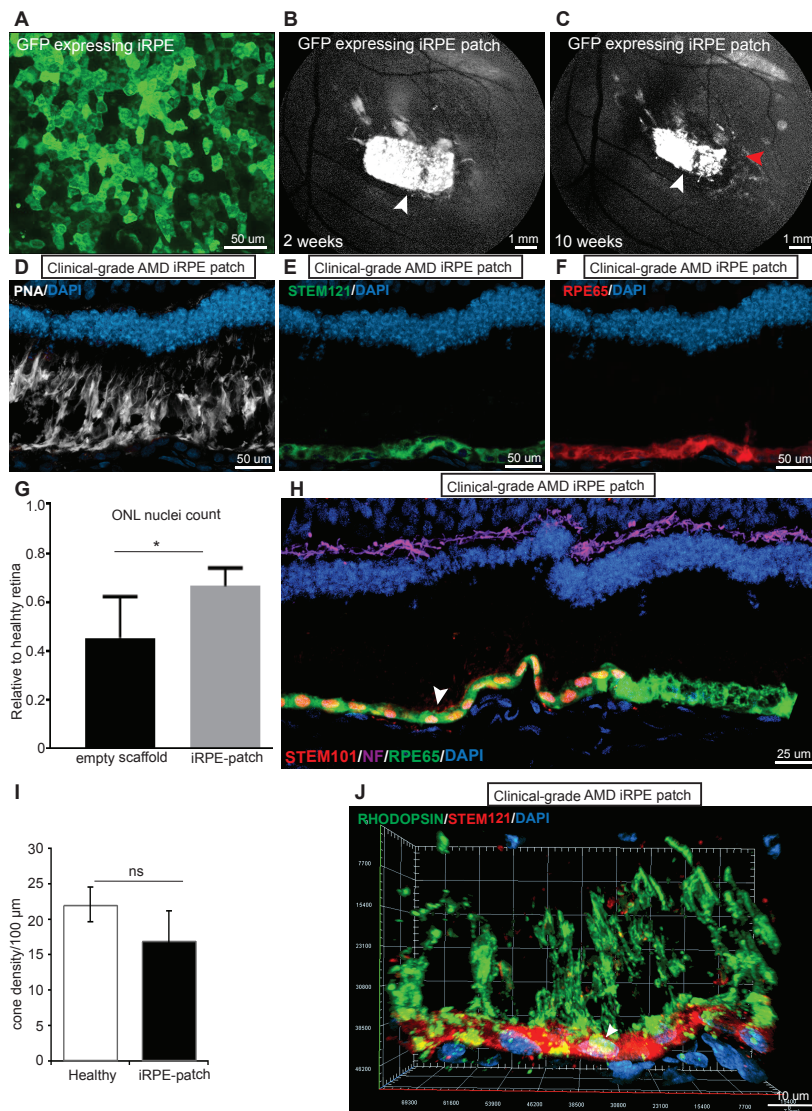


Fig. S8. Analysis of iRPE-patch in pig model of laser-induced retinal degeneration. (A) GFP expressing human iRPE-patch. (B, C) Fundus autofluorescence images showing GFP-positive 4x2 mm iRPE-patch under the retina 2 weeks (white arrowhead) and 10 weeks post-transplantation (white arrowhead shows the iRPE-patch and red arrowhead shows the laser area). Note, human cells do not migrate away from the patch. (D-F) Images of human iRPE-patch transplanted area of pig retina stained for photoreceptors (PNA, white, D); and immunostained for human iRPE cells (STEM121, green, E) and RPE (RPE65, red, F). (G) Quantification of the number of nuclei in the outer nuclear layer (ONL) of pig retina above the area of empty scaffold as compared to the area of iRPE-patch. Numbers are presented as fraction of healthy retina. * $p < 0.05$ determined using two-tailed t-test. (H) Immunostaining for human nuclear antigen STEM101 (red) and RPE65 (green) confirms integration of human iRPE-patch in the pig eye. (I) Quantification of the number of cones in healthy pig retina as compared to the area above the iRPE-patch. Numbers are presented as fraction of healthy retina. p -value healthy-iRPE-patch = 0.145 determined using two-tailed t-test. (J) 3D reconstruction of Rhodopsin (green) and STEM121 (red) (white arrowheads) immunostained sections of human iRPE-patch transplanted in a pig eye shows photoreceptor outer segments (POS) inside human RPE cells.

Supplementary Figure 9

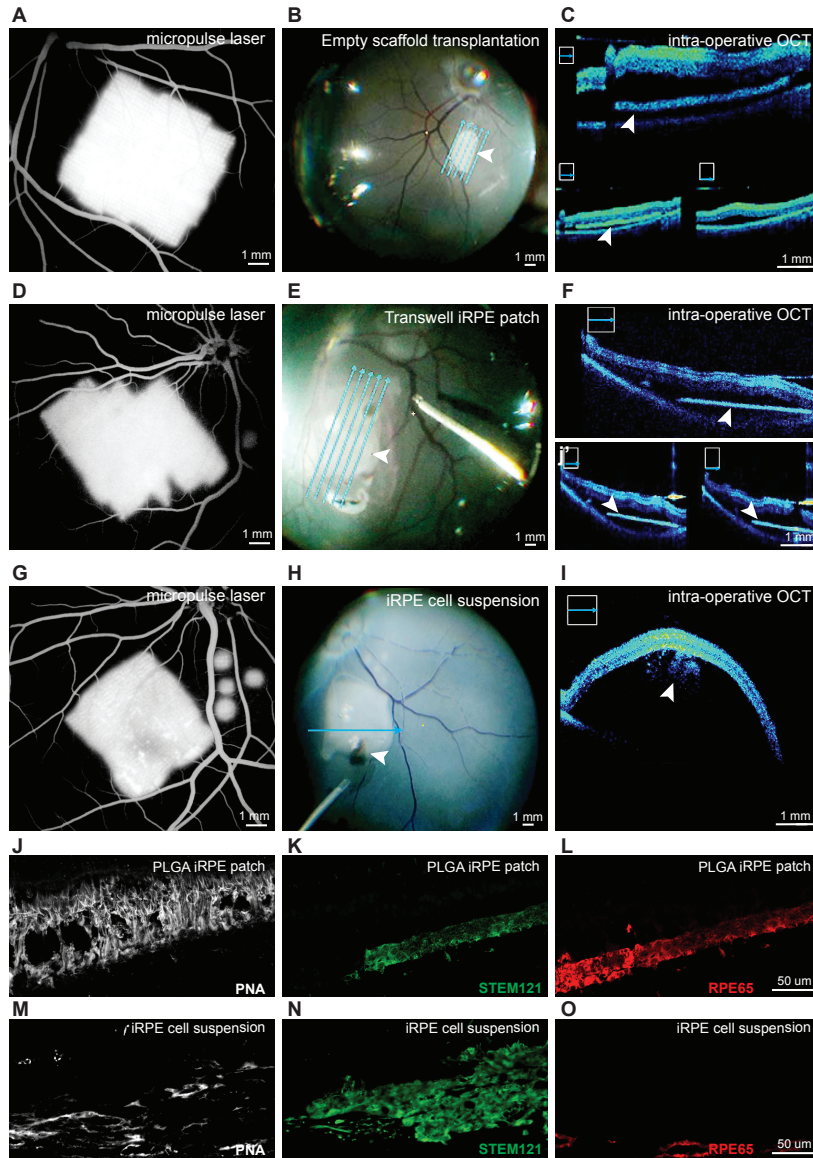


Fig. S9. Comparative efficacy analysis of iRPE patch and iRPE suspension in the pig model. (A-I)

Fluorescein angiography (**A, D, G**) confirming micropulse laser based RPE-injury in pig eyes used for empty scaffold (**A**), transwell-iRPE-patch (**D**), and iRPE cell injection (**G**) transplantation. Intra-operative fundus imaging (**B, E, H**), and intra-operative OCT (**C, F, I**) confirming correct delivery of empty scaffold (**B, C**), transwell-iRPE-patch (**E, F**), and iRPE cell injection (**H, I**). White arrowheads mark the various transplants. (**J-L**) Images of human iRPE-patch transplanted area of pig retina stained for photoreceptors (PNA, white, **J**); and immunostained for human iRPE cells (STEM121, green, **K**) and RPE (RPE65, red, **L**). Note, STEM121 label for human cells (see underlined in **K**) stops where the pig RPE begins.

Table S1: Validation of clinical (GMP)-grade iPSC Working Bank derived from CD34+ cells. iPSC Working Banks at passage 10 were validated for being sterile (free of bacteria, fungus, and mycoplasma); normal G-band karyotyping; expression of pluripotency markers (SSEA4, TRA1-60, TRA1-81, and OCT4 positivity); percent cells that have lost the reprogramming plasmid; identity of iPSCs with patient material

	Age	Pheno- type	Clone	Sterility/ mycoplasma	Karyotype*/ Gender	% ve SSEA4 ⁺ cells	% ve TRA1-60 ⁺ cells	% ve TRA1-81 ⁺ cells	% ve OCT4 ⁺ cells	% Cells with plasmid loss	STR analysis PBMC=iPSC (patient match)	Onco- gene sequence (patient match)
2	85	Bilateral GA	A	UD	Normal 46/XY	99.3	99.03	99.80	99.94	100	matched	matched
			B	UD	Normal 46/XY	99.50	100	100	100	100	matched	Several mis-match
			C	UD	Normal 46/XY	99.56	99.56	100	99	100	matched	matched
3	89	Bilateral GA	A	UD	Normal 46/XY	99.25	99.97	100.00	99.96	100	matched	matched
			C	UD	Normal 46/XY	99.24	100	99.95	100	100	matched	matched
			D	UD	Normal 46/XY	99.25	99.97	100.00	99.96	100	matched	matched
4	87	Bilateral GA	A	UD	Normal 46/XX	99.8	100	100	99.96	100	matched	matched
			B	UD	Normal 46/XX	99.38	100	100	99.96	100	matched	matched
			C	UD	Normal 46/XX	99.8	100	100	99.96	100	matched	matched

UD = undetectable. Sterility was tested at WuXi AppTec; G-band Karyotyping and STR analysis was performed at Cell Line Genetics; Plasmid loss was detected using a fluidigm single cell qPCR assay at Cellular Dynamics International, Inc.

Table S2

Oncogene exome analysis of iPSC vs donor PBMCs

- 1590_101, no cancerous mutations in clone
- 1590_103, no cancerous mutations in clone
- 1590_104, no cancerous mutations in clone; seven sequence changes in clone
- 1592_101, no cancerous mutations in clone; one heterozygous splicing change in DNTM3A. This variant is present at a frequency of 0.012 (43 / 3743) in the PBMC donor.
- 1592_122, no cancerous mutations in clone
- 1592_123, no cancerous mutations in clone
- 1620_102, no cancerous mutations in clone; one variant with a one base pair deletion with 0.0261 frequency in the clone and 0.0268 frequency in the donor PBMC
- 1620_104, no cancerous mutations in clone

TUTE predicted deleterious mutations novel in the clones

1590_101, no cancerous mutations in clone

Show entries Code

Search:

CHROM	POS	REF	ALT	GT.x	GT.y	AF.x	AF.y	DP.x	INFO.x
No data available in table									

Showing 0 to 0 of 0 entries Previous Next

1590_103, no cancerous mutations in clone

Show entries Code

Search:

CHROM	POS	REF	ALT	GT.x	GT.y	AF.x	AF.y	DP.x	INFO.x
No data available in table									

Showing 0 to 0 of 0 entries Previous Next

1590_104, no cancerous mutations in clone; seven new changes in clone

Show entries Code

Search:

Table S2 contd.

	CHROM	POS	REF	ALT	GT _x	GT _y	AF _x	AF _y	DP _x	
1	1	156848918	C	T	011		0.441		4358	VC=SNV;Func=exonic;Gene=NTRK1;ExonicFunc=missense;FullAA=NTRK1;NM_001123385.1;ClinVar=Pathogenic;ClinVar_Dis= Familial medullary thyroid carcinoma;Hereditary_inse
2	14	81606214	A	G	011		0.238		4195	VC=SNV;Func=splicing;Gene=TSFR;Transcript=NM_000369.2;NucleotideChange=
3	16	89842176	C	G	011		0.196		3007	VC=SNV;Func=exonic;Gene=FANCA;ExonicFunc=missense;FullAA=FANCA;NM_000061.4
4	3	189455550	T	G	011		0.205		4929	VC=SNV;Func=exonic;Gene=TP63;ExonicFunc=missense;FullAA=TP63;NM_001111111.1
5	4	55129831	C	T	011		0.184		3848	VC=SNV;Func=splicing;Gene=PDGFRA;Transcript=NM_006206.4;NucleotideChange=
6	7	140434574	C	CA	011		0.18		1314	VC=INDEL;Func=splicing;Gene=BRAF;Transcript=NM_004333.4;NucleotideChange=
7	X	39911657	C	A	011		0.298		1758	VC=SNV;Func=splicing;Gene=BCOR;Transcript=NM_001123385.1;NucleotideChange=

Showing 1 to 7 of 7 entries

Previous Next

1592_101, no cancerous mutations in clone; one heterozygous splicing change in DNMT3A. This variant is present at a frequency of 0.012 (43 / 3743) in the PBMC donor.

Show entries

Search:

	CHROM	POS	REF	ALT	GT _x	GT _y	AF _x	AF _y	DP _x	
1	2	25470029	T	C	011		0.499		5439	VC=SNV;Func=splicing;Gene=DNMT3A;Transcript=NM_175629.2;NucleotideChange=2A>C;MutTaster=1.000;MutTaster_Pred=D;GERP+_RS=4.0;phyloP46way_placenta

Showing 1 to 1 of 1 entries

Previous Next

1592_122, no cancerous mutations in clone

Show entries

Search:

	CHROM	POS	REF	ALT	GT _x	GT _y	AF _x	AF _y	DP _x	INFO _x
No data available in table										

Showing 0 to 0 of 0 entries

Previous Next

1592_123, no cancerous mutations in clone

Show entries

Search:

	CHROM	POS	REF	ALT	GT _x	GT _y	AF _x	AF _y	DP _x	INFO _x
No data available in table										

Table S2 contd..

Showing 0 to 0 of 0 entries

[Previous](#) [Next](#)

1620_102, no cancerous mutations in clone; one variant with a one base pair deletion with 0.0261 frequency in the clone and 0.0268 frequency in the donor PBMC

Show entries

Search:

[Code](#)

CHROM	POS	REF	ALT	GT _x	GT _y	AF _x	AF _y	DP _x	INFO _x
1	5	131931451	TA	T	0 1	0.0261		2945	VC=INDEL;Func=exonic;Gene=RAD50;ExonicFunc=frame shift;FullAA=RAD50:NM_005732.3:exon13:c.2157delA;p.L719fs;Transcript=NM_0

Showing 1 to 1 of 1 entries

[Previous](#) [Next](#)

1620_104, no cancerous mutations in clone

Show entries

Search:

[Code](#)

CHROM	POS	REF	ALT	GT _x	GT _y	AF _x	AF _y	DP _x	INFO _x
No data available in table									

Showing 0 to 0 of 0 entries

[Previous](#) [Next](#)

Table S3

Detailed list of clinical-grade reagents used in iPSC generation and RPE differentiation

Reagents	Vendor	Catalogue	Use description
Plasmid 149	Aldevron	p149	Reprogramming
Plasmid 150	Aldevron	p150	Reprogramming
ViCell concentration control 8X106 Beads/mL	Beckman Coulter	B78897	Differentiation
CryoStor CS10	BioLife Solutions	210102	Ficoll/Reprogramming/Differentiation
TPO 50 ug	CellGenix	1017-050	Reprogramming
triCitrasol	Citra Labs	PN6030	Ficoll
Fetal Bovine Serum (U.S.), Characterized	GE Healthcare (Hyclone)	SH30071.03	Differentiation
DNase I (PULMOZYME) (2 ug in 2 mL)	Genentech	50242-100-040 10039	Reprogramming
Lymphocyte Separation Medium	Lonza/corning	17-829E/25- 072-C1	Ficoll
CD34 Nucleofactor® Solution	Lonza	VPA-1003	Reprogramming
CD34 Nucleofactor® Supplement	Lonza	VPA-1003	Reprogramming
DPBS without Ca ⁺⁺ and Mg ⁺⁺	Lonza/Life Technology	17- 512F/14190250	Ficoll/Reprogramming/Differentiation
Versene Solution	Thermo Fisher	15040-066	Reprogramming/Differentiation
Recombinant hLIF (10 ug/ml)	Millipore	LIF1010	Reprogramming
H-1152 (1 mg)	Millipore	555550	Differentiation
CliniMACS® PBS/EDTA Buffer	Miltenyi Biotec	700-25	Reprogramming
CliniMACs CD34+ microbeads	Miltenyi Biotec	171-01	Reprogramming
CliniMACS CD56 microbeads	Miltenyi Biotec	130-019-401	Differentiation
CliniMACS Anti-Biotin microbeads	Miltenyi Biotec	130-019-201	Differentiation
Mouse Anti-CD24 (Biotin Conjugated)	Miltenyi Biotec	Custom made	Differentiation
DMSO	Mylan Institutional	67457-178-10	Reprogramming/Differentiation
Flt-3 (50ug)	R&D Systems	308-GMP-050	Reprogramming
SCF (50ug)	R&D Systems	255-GMP-050	Reprogramming
IL-6 (50ug)	R&D Systems	206-GMP-050	Reprogramming
IL-3 (50ug)	R&D Systems	203-GMP-050	Reprogramming
Recombinant Human Activin A, Animal-Free (60 ug, 645 ul /vial, 0.094 mg/ml) CUSTOM VIALED	R&D Systems	AFL 338	Differentiation
Recombinant Human IGF-I, Animal-Free (5.5 ug, 55 uL)- CUSTOM VIALED	R&D Systems	291-GMP- 5.5ug	Differentiation
PGE2 (10 mg)	R&D Systems	2296	Differentiation

Table S3 contd..

SB431542 Hydrate (10 mg)	R&D Systems	1614	Differentiation
Blebbistatin (5 mg)	Sigma Aldrich	B0560	Differentiation
Ascorbic Acid (2 g)	Sigma Aldrich	PHR1008-2G	Differentiation
CKI-7 Dihydrochloride (5 mg)	Sigma Aldrich	C0742-5mg	Differentiation
Niacinamide (1g)	Sigma Aldrich	PHR1033-1G	Differentiation
Taurine (1g)	Sigma Aldrich	PHR1109-1G	Differentiation
Hydrocortisone (50 uM)	Sigma Aldrich	H-6909	Differentiation
3,3',5-Triiodo-L-thyronine sodium salt (1 mg)	Sigma Aldrich	T5516	Differentiation
Y-27632 (1mg)	Sigma Aldrich	Y0503-1MG	Reprogramming
Beta-Mercaptoethanol	Sigma Aldrich	07604	Reprogramming
HA-100 (5 mg)	StemCell Technologies	72482	Reprogramming
StemSpan ACF	StemCell Technologies	09805	Reprogramming
CHIR99021 (2 mg)	Stemgent	04-0004-02	Reprogramming
A-83-01 (2 mg)	Stemgent	04-0014	Reprogramming
LDN-193189 (10 mg)	Stemgent	04-0074-10	Differentiation
PD325901 (2mg)	Stemgent	04-0006	Differentiation
Retronectin (2.5 mg)	Takara	T202	Reprogramming
UltraPure 0.5M EDTA, pH 8	Thermo Fisher	15575-020	Differentiation
CTS N2 Supplement (100 X)	Thermo Fisher	A13707-01	Reprogramming/Differentiation
100x Glutamax	Thermo Fisher	35050-061	Reprogramming
E8 Basal medium	Thermo Fisher	A15169-01	Reprogramming/Differentiation
E8 supplement	Thermo Fisher	A15170-01	Reprogramming
CTS Vitronectin (VTN-N)	Thermo Fisher	A27940	Reprogramming/Differentiation
DMEM/F12, HEPES	Thermo Fisher	11330-032	Reprogramming/Differentiation
MEM Alpha, nucleosides	Thermo Fisher	12571-063	Differentiation
MEM non-essential AA	Thermo Fisher	11140-050	Differentiation
Sodium Pyruvate (100 mM)	Thermo Fisher	11360-070	Differentiation
CTS KnockOut™ SR XenoFree	Thermo Fisher	A1099201	Differentiation
B-27 Supplement 50 X, Serum free	Thermo Fisher	17504-044	Differentiation
CTS TrypLE Select Enzyme	Thermo Fisher	A12859-01	Reprogramming/Differentiation
Water for injection (WFI)	APP Pharmaceuticals	NDC-63323-185-10	Reprogramming/Differentiation
CTS B-27 Supplement, XenoFree	Thermo Fisher	A14867-01	Reprogramming
Recombinant human FGF2 (0.1 mg/ml)	Waisman Biomanufacturing	WC-FGF2-FP-003	Reprogramming
10 M NaOH	Sigma Aldrich	72068	Differentiation
ViCell Reagent Pack	Beckman Coulter	383722	Differentiation

Certificate of Analysis for all reagents have been validated for all these reagents for our clinical-grade manufacturing processes.

Table S4: Summary of Body Weight Change in Rats Transplanted with iPSC-derived RPE

Days		Weekly body weight (grams)									
		1	8	15	22	29	36	43	50	57	64
Vehicle control*	Mean	234	234	254	272	283	290	295	304	309	316
	SD	24.0	26.1	26.2	24.5	28.7	25.1	27.0	27.3	30.8	30.6
iPSC-RPE sheet*	Mean	233	233	250	273	285	293	289	294	292	303
	SD	19.6	20.9	21.8	23.6	25.7	27.8	27.8	30.9	33.3	31.2
iPSC-RPE suspension*	Mean	270	270	283	273	288	296	303	304	307	315
	SD	29.0	26.8	24.9	27.2	25.3	24.9	26.7	26.0	28.3	29.3

*overall p-value (p>0.1) determined using ANOVA and Dunnett's test

Summary of Daily Food Consumption in Rats Transplanted with iPSC-derived RPE

Days		Food consumption (grams/animal/day)									
		1-8	8-15	15-22	22-29	29-36	36-43	43-50	50-57	57-64	64-71
Vehicle control*	Mean	17	16	19	18	19	18	18	18	18	18
	SD	0.7	1.5	2.1	1.3	1.2	1.7	1.8	1.0	1.3	1.2
iPSC-RPE sheet*	Mean	16	17	20	19	19	17	18	17	18	19
	SD	2.6	1.3	1.3	1.2	1.4	1.0	1.4	0.8	1.2	1.0
iPSC-RPE suspension*	Mean	17	17	19	18	18	17	17	18	18	17
	SD	0.9	1.3	3.0	1.0	1.3	1.0	1.1	1.2	0.9	1.0

*overall p-value (p>0.1) determined using ANOVA and Dunnett's test

Table S4. Lactic acid released by the PLGA scaffold during degradation. Days 1-35 are the in vitro stage of the scaffold and days 35 onwards are in vivo after transplantation. Grey highlights the days of PLGA scaffold bulk degradation phase (days 19-36). Note, the bulk degradation of the scaffold occurs in vitro.

	Samples	mmol/L/scaffold/day	percent lactic acid released/scaffold/week
In vitro stage of iPSC-RPE-patch maturation	1-1 to 1-6 (days 1-6)	0.00047±0.00016	4.2%±1.7%
	2-1 to 2-6 (days 7-12)	0.00047±0.00016	4.2%±1.7%
	3-1 to 3-6 (days 13-18)	0.00047±0.00016	4.2%±1.7%
	4-1 to 4-6 (days 19-24)	0.00297±0.00056	31.9%±4.0%
	5-1 to 5-6 (days 25-30)	0.00273±0.00069	29.4%±7.5%
	6-1 to 6-6 (days 31-36)	0.00089±0.00048	9.6%±4.9%
In vitro stage of iPSC-RPE-patch after transplantation in the sub-retinal space	7-1 to 7-6 (days 37-42)	0.00047±0.00016	4.2%±1.7%
	8-1 to 8-6 (days 43-48)	0.00047±0.00016	4.2%±1.7%
	9-1 to 9-6 (days 48-54)	0.00047±0.00016	4.2%±1.7%
	10-1 to 10-6 (days 54-60)	0.00047±0.00016	4.2%±1.7%

Image Replicates for Figure 2

Figure 2C - second replicates

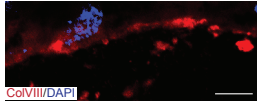
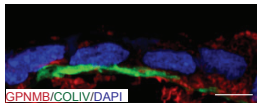
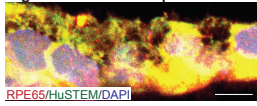


Figure 2C - third replicates

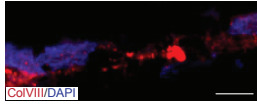
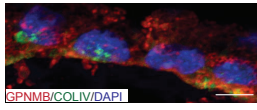
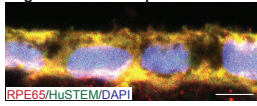


Figure 2D - second replicates

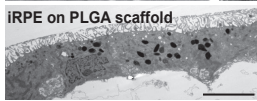
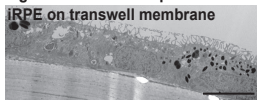


Figure 2D - third replicates

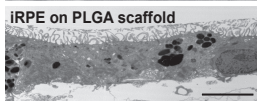
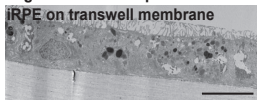


Image Replicates for Figure 3

Figure 3A,B - second replicate

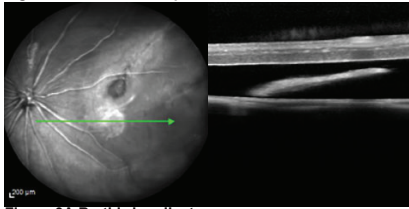


Figure 3A,B - third replicate

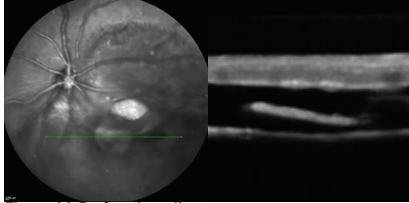


Figure 3A,B - fourth replicate

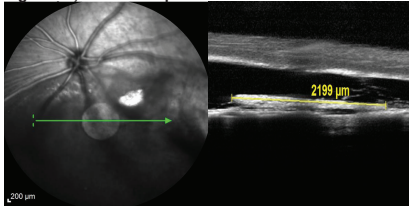


Figure 3C - second replicate

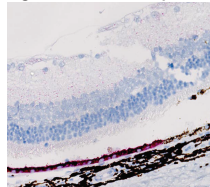


Figure 3C - third replicate

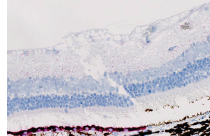


Figure 3C - fourth replicate

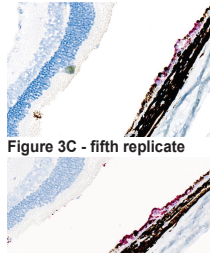


Figure 3C - fifth replicate

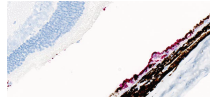


Figure 3C - sixth replicate

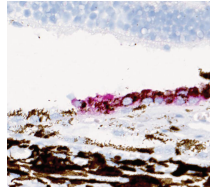


Figure 3C - seventh replicate



Figure 3C - eighth replicate

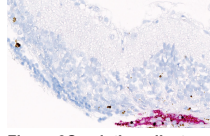


Figure 3C - ninth replicate



Figure 3C - tenth replicate



Figure 3D-E - second replicate

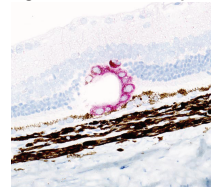


Figure 3D-E - third replicate

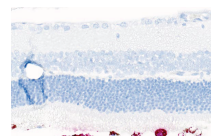


Figure 3D-E - fourth replicate

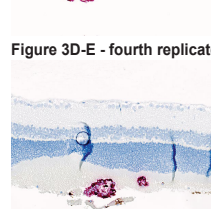


Figure 3D-E - fifth replicate

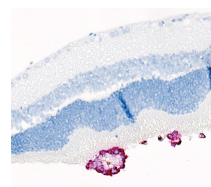


Figure 3D-E - sixth replicate

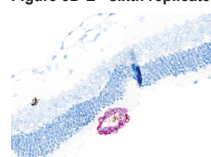


Figure 3D-E - seventh replicate

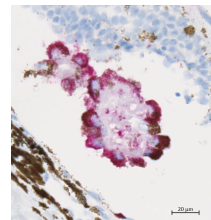


Figure 3F - second replicate

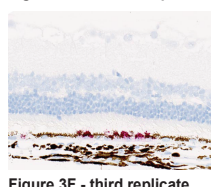


Figure 3F - third replicate



Figure 3F - fourth replicate

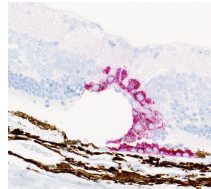


Figure 3F - fifth replicate

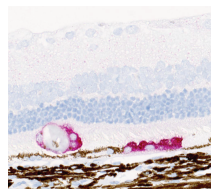


Figure 3F - sixth replicate

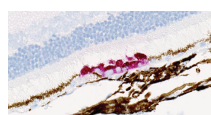


Figure 3F - seventh replicate

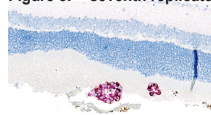


Figure 3D-F - eighth replicate

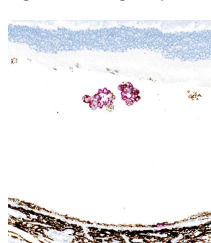


Image Replicates for Figure 4

Figure 4B- second replicate

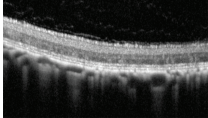


Figure 4C- second replicate

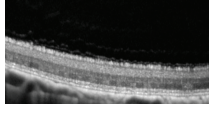


Figure 4B- third replicate

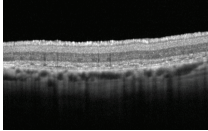


Figure 4C- third replicate

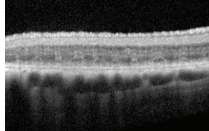


Figure 4H - second replicate

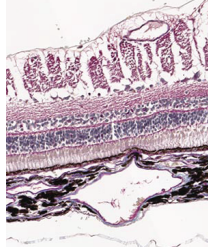


Figure 4H- third replicate

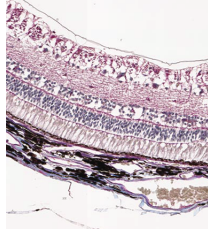


Figure 4I - second replicate

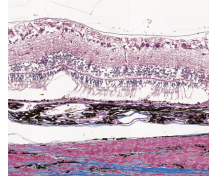


Image Replicates for Figure 5

Figure 5A- second replicate

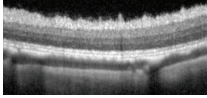


Figure 5B- second replicate

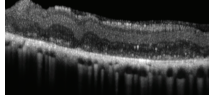


Figure 5C - second replicate

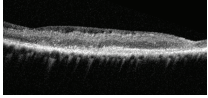


Figure 5A- third replicate

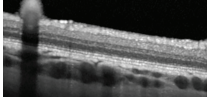


Figure 5B- third replicate

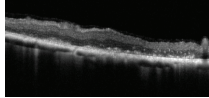


Figure 5C- third replicate

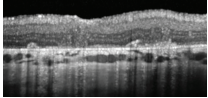


Figure 5D- second replicate

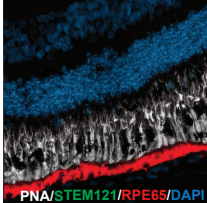


Figure 5D- third replicate

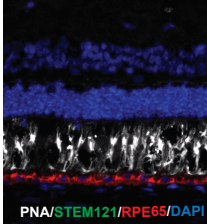


Figure 5E- second replicate

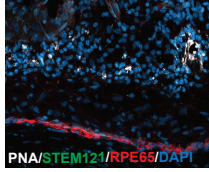


Figure 5E- third replicate

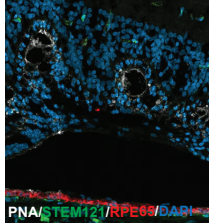


Figure 5F - second replicate

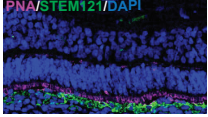


Figure 5F- third replicate

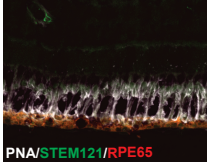


Image Replicates for Figure 6

